Preliminary Design of the Two-Phase Ejector under Constant Area Mixing Assumption for 5 kW Experimental System

Ayşe Uğurcan Atmaca[1,*], *Aytunç Erek*[1], and *Orhan Ekren*[2]

[1]Dokuz Eylül University, Faculty of Engineering, Mechanical Engineering Department, Tınaztepe Yerleşkesi 35397 Buca, İzmir, Turkey
[2]Ege University, Solar Energy Institute, 35100 Bornova, İzmir, Turkey

Abstract. Ejector expansion refrigeration cycle is the modification of the vapour compression refrigeration cycle with the implementation of a two-phase ejector and a vapour-liquid separator to improve the cycle performance. In this study, main geometrical parameters of an ejector, i.e. diameters of the motive nozzle throat, motive nozzle outlet, suction nozzle outlet, and constant area mixing section are calculated in order to provide the preliminary design aspects at various operation conditions. The thermodynamic model of the ejector is established with reference to constant-area mixing assumption. The equations are solved in Matlab®. The environmentally-friendly refrigerants, R1234yf and R1234ze(E) from the hydrofluoroolefins (HFOs) and R134a which is about to be phased out by the F-gas Regulation are used in the analyses. When compared to the previous literature findings, the current research aims to compare the dimensions of a two-phase ejector to be used in an experimental system having 5 kW cooling capacity for these three refrigerants.

1 Introduction

Use of ejectors to recover the throttling losses in the vapor compression refrigeration cycle (VCRC) dates back to the patent of Gay in 1931 proposing a two-phase ejector instead of the expansion valve in order to improve the cycle performance [1]. Schematic view of the ejector expansion refrigeration cycle (EERC) and basic ejector sections, namely motive (primary) nozzle, suction (secondary) nozzle (chamber), mixing section, and diffuser, are shown in Fig. 1 and Fig. 2, respectively.

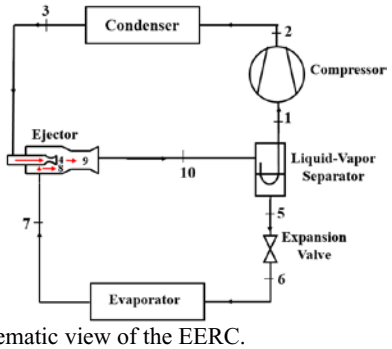

Fig. 1. Schematic view of the EERC.

Thermodynamic models of the ejectors are commonly established in order to evaluate the cycle performance. Zero-dimensional (0D) thermodynamic models are constructed with respect to two types of mixing theories, i.e. constant-pressure mixing (CPM) and constant-area mixing (CAM) ejectors [2]. Kornhauser [3] established the thermodynamic equations of the CPM ejector and Li and Groll [4] constructed the EERC model with respect to the CAM approach for the first time. Coefficient of performance (COP), pressure lift ratio, entrainment ratio, and area ratio could be calculated through medium of above-mentioned 0D thermodynamic models [3, 4].

Thermodynamic models could provide limited geometrical parameters regarding the design of the ejector. The basic geometrical parameters, i.e. motive nozzle throat diameter, motive nozzle outlet diameter, suction nozzle outlet diameter, and constant-area section diameter could be calculated making use of thermodynamic models. Benefiting from the previous experimental analyses [5-7], other dimensions concerned with the lengths of the ejector sections as well could be determined using the length to diameter ratio values [8].

Modelling approaches of Hassanain et al. [8] and Sherif et al. [9] are used to determine the basic geometrical diameters of a two-phase ejector to be used in the EERC having 5 kW cooling/refrigeration capacity. However, the model of this present paper doesn't include the total mass flow rate among the inputs. Moreover, as one of the main target of this research, environmentally-friendly refrigerant alternatives having low-global warming potential (GWP), R1234yf and R1234ze(E) are intended to be compared from the design viewpoint and also R134a which is about to be prohibited by F-gas Regulation [10] is added to the list to extend the comparative gains from this paper.

Atmaca et al. [11] previously made thermodynamic analyses on the EERC for environmentally-friendly refrigerant alternatives at various operating conditions. Benefiting from the outcomes of Atmaca et al. [11],

* Corresponding author: ugurcan.atmaca@deu.edu.tr

optimum values of the entrainment ratios, suction nozzle pressures, and enthalpy differences through the evaporator at various operating conditions under constant-area mixing assumption are used to calculate the specified diameters of the two-phase ejector for a 5 kW experimental system. Modelling equations for the diameters of the two-phase ejector are solved in Matlab®. Thermodynamic properties of the refrigerants are determined using REFPROP version 9.1 [12]. As of the outline, Section 2 explains ejector models based on the mixing assumptions and Section 3 presents equations for the geometrical parameter calculations. Finally, Section 4 displays and discusses the results.

2 Ejector models based on the mixing assumptions

Thermodynamic models of the ejectors are presented according to two kinds of assumptions as CAM and CPM. In CAM theory, the mixing process of the primary and secondary fluid flows occurs in the constant-area section and the pressure of the total flow increases as a result of the mixing; whereas in the CPM theory, the mixing process occurs in a kind of geometry enabling constant pressure mixing, hence the pressure stays the same throughout mixing [3, 4].

Main outputs of this paper are defined according to both configurations of CAM ejector given in Fig. 2 and they are calculated in the same way for both of the schematics under the modelling assumptions of this paper. CPM ejector template as well is defined with reference to Sherif et al. [9] as given in Fig. 3.

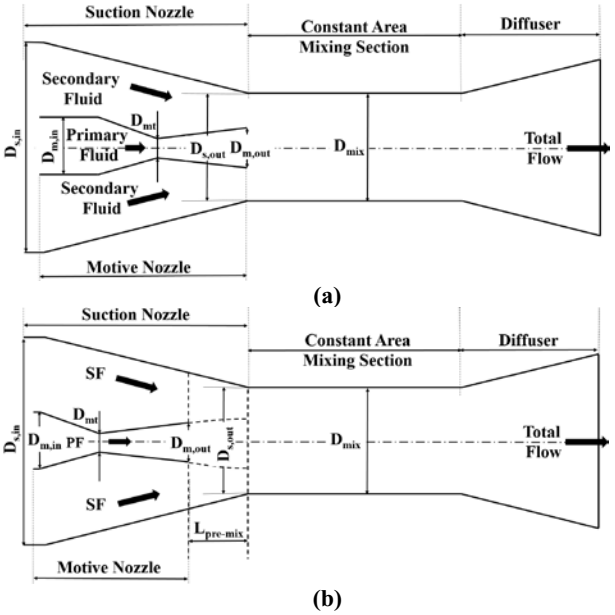

Fig. 2. Design parameters of a CAM ejector with the motive nozzle outlet coinciding with the constant area inlet section **(a)** and motive nozzle outlet located within the suction nozzle including a pre-mixing chamber **(b)** (PF: primary fluid, SF: secondary fluid).

According to the thermodynamic analyses of Atmaca et al. [11], CAM theory results in slightly higher performance at the optimum suction nozzle pressure when compared to CPM assumption and the main conclusion is that they are just modelling assumptions. Hence, both of them could be used in the thermodynamic models for performance estimations. However, when geometrical parameter definition is the issue, choice of the ejector mixing assumption makes a difference as seen from Fig. 2 and Fig. 3.

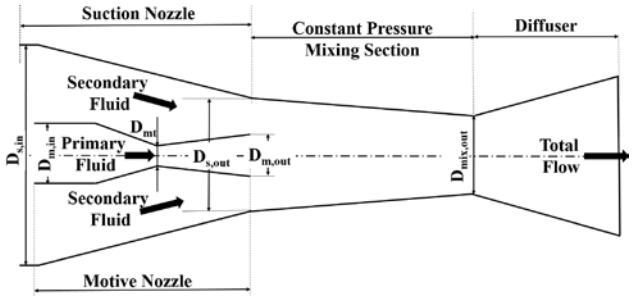

Fig. 3. Design parameters of a CPM ejector.

3 Thermodynamic modelling

There are typical assumptions regarding both the ejector and cycle modelling. These assumptions were defined mainly with reference to Li and Groll and Kornhauser [3, 4]. Thermodynamic modelling equations for the expansion, mixing, and compression processes within the ejector is described with reference to Li and Groll [4] under constant area mixing assumption. Entrainment ratio which is the ratio of the secondary fluid mass flow rate to the motive fluid mass flow rate as described below is a critical parameter expected to be as high as possible for a well-designed ejector.

$$w = \frac{\dot{m}_s}{\dot{m}_m} \tag{1}$$

Equations for the primary dimension calculations are established in main with reference to Hassanain et al. [8]. First of all, mass flow rate of the secondary flow is determined in accordance with the defined cooling capacity and the enthalpy difference through the evaporator for the optimum suction nozzle pressure at the investigated operating temperatures. Subsequently, the primary fluid mass flow rate is calculated from the optimum entrainment ratio. Mass flow rates of the primary and secondary fluids are calculated as follows;

$$\dot{m}_s = \frac{\dot{Q}_e}{\Delta h_{e,opt}} \tag{2}$$

$$\dot{m}_m = \frac{\dot{m}_s}{w_{opt}} \tag{3}$$

Secondly, the throat pressure, P_{mt} is calculated iteratively. The difference between the sound velocity at the estimated throat pressure and calculated velocity

from the energy equation is compared and iterations are repeated until the calculated velocity and sound velocity values at the throat converge each other within an acceptable error range since Mach number at the throat must be equal to unity. Sound velocity [13] and void fraction for homogeneous flow (V_g/V_l=1) [14] is given as

$$c = \left[\rho_{tp} \left(\frac{\alpha}{\rho_g c_g^2} + \frac{1-\alpha}{\rho_l c_l^2} \right) \right]^{-1/2} \quad (4)$$

$$\rho_{tp} = \alpha \rho_g + (1-\alpha)\rho_l \quad (5)$$

$$\alpha = \frac{X_m}{X_m + (1-X_m)\frac{\rho_g}{\rho_l}} \quad (6)$$

Density of the two-phase flow calculated from Equation (5) is the same as the value obtained from REFPROP program [12]. By the way, efficiency of the converging and diverging sections of the motive nozzle is assumed to be the same for the nozzle efficiency. Throat velocity calculated from the energy equation is given as

$$h_{mt} = (1-\eta_m) h_{m,in} + \eta_m h(s_{m,in}, P_{mt}) \quad (7)$$

$$u_{mt} = \sqrt{2(h_{m,in} - h_{mt}) + u_{m,in}^2} \quad (8)$$

When the exact throat pressure is estimated iteratively, the throat diameter is calculated as follows;

$$D_{mt} = \sqrt{\frac{4\dot{m}_m}{\pi \rho_{mt} u_{mt}}} \quad (9)$$

Motive nozzle outlet and suction nozzle outlet diameters are calculated according to the optimum expansion pressure at the outlets. Constant-area mixing section diameter is the same as the suction nozzle diameter. The formulation is given separately for these two sections, but it is already known from the assumptions and templates of Fig. 2 that they are equal for 100% efficient mixing process. The expressions for the diameters of a constant-area mixing ejector are as

$$D_{m,out} = \sqrt{\frac{4\dot{m}_m}{\pi \rho_{m,out} u_{m,out}}} \quad (10)$$

$$D_{s,out} = \sqrt{\frac{4\dot{m}_s}{\pi \rho_{s,out} u_{s,out}} + D_{m,out}^2} \quad (11)$$

$$D_{mix} = \sqrt{\frac{4(\dot{m}_m + \dot{m}_s)}{\pi \rho_{mix,out} u_{mix,out}}} \quad (12)$$

4 Results and discussion

Inputs of the thermodynamic analyses are presented in Table 1. They are typically for an air-conditioning application. First of all, the variation of w_{opt} and $P_{s,opt}$ are displayed with respect to various evaporator and condenser temperatures as shown in Fig. 4. These variations are presented with reference to the modelling results of Atmaca et al. [11]. In Fig. 5 enthalpy difference through the evaporator at the optimum suction nozzle pressure is presented for the same operating points. In Fig. 6, mass flow rates of the primary and secondary fluid flows are shown. The highest mass flows are calculated for R1234yf due to the lowest enthalpy difference values at the investigated operating points. R1234ze(E) and R134a yielded closer mass flow rates for the primary and secondary fluids.

Table 1. Operating conditions for the thermodynamic analyses.

Parameters	Values
Evaporator temperature (T_e)	5 ˚C
Evaporator outlet superheat temperature difference (ΔT_{sh})	5 K
Condenser Temperature (T_c)	40 ˚C
Condenser outlet subcooling temperature difference (ΔT_{sc})	3 K
Compressor efficiency (η_{comp})	0.75
Primary nozzle efficiency (η_m)	0.9
Suction nozzle efficiency (η_s)	0.9
Diffusor efficiency (η_d)	0.8
Cooling (Refrigeration) capacity (kW)	5
$D_{s,in}$ (mm)	60
$D_{m,in}$ (mm)	15

Secondary fluid mass flows have lower rate of change (around 4-5%) for three of the refrigerants according to evaporation temperature as obvious from Fig. 6 (a). On the other hand, rate of change varies more (7-9%) for the primary fluid mass flow rate at the same evaporation temperature range. Primary fluid mass flow rate decreases according to the increased evaporator temperature; whereas secondary fluid mass flow rate increases. When condenser temperature is increased, mass flow rates of the primary and secondary fluids increase as shown in Fig. 6 (b). Fig. 7 shows the variation of the motive nozzle throat and outlet diameters according to the evaporator and condenser temperatures. As shown from Fig. 7 (a) and (b), motive nozzle outlet diameter is affected mostly by the changes in the evaporator temperature since the optimum suction nozzle pressure reacts more to the changes in the evaporator temperature.

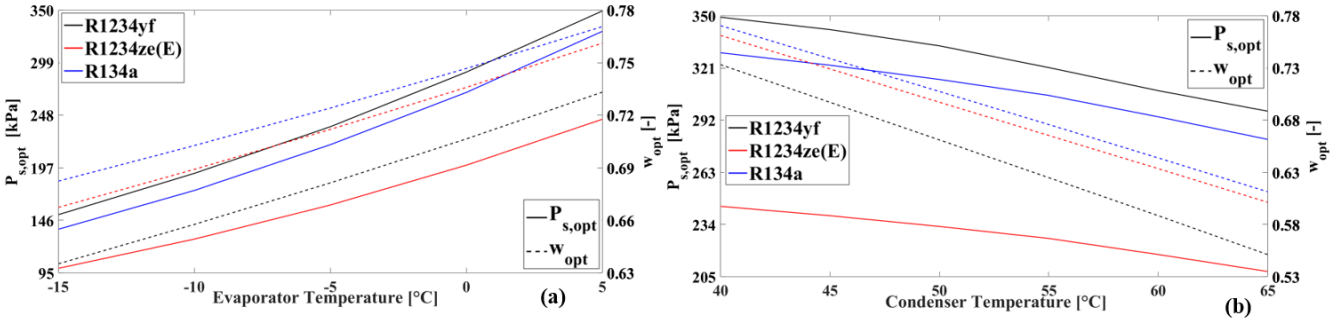

Fig. 4. Variation of the optimum suction pressure and entrainment ratio according to the evaporator **(a)** and condenser **(b)** temperatures.

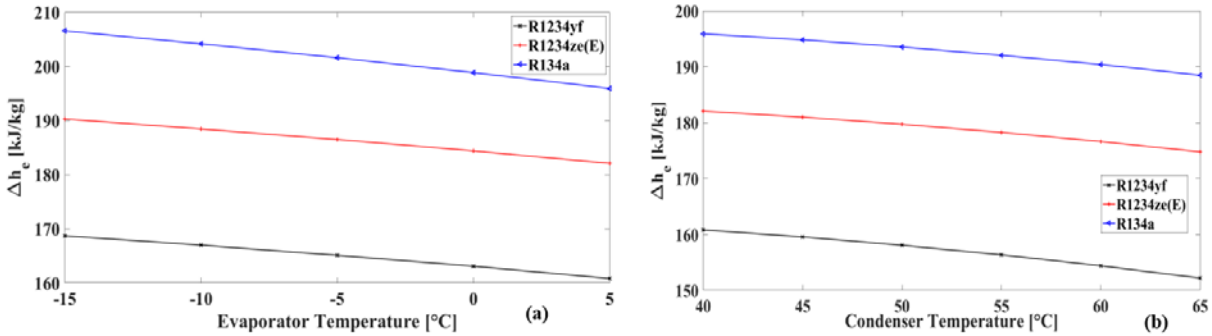

Fig. 5. Variation of the evaporator enthalpy difference at the optimum suction nozzle pressure for the ejector design with respect to the evaporator **(a)** and condenser **(b)** temperatures.

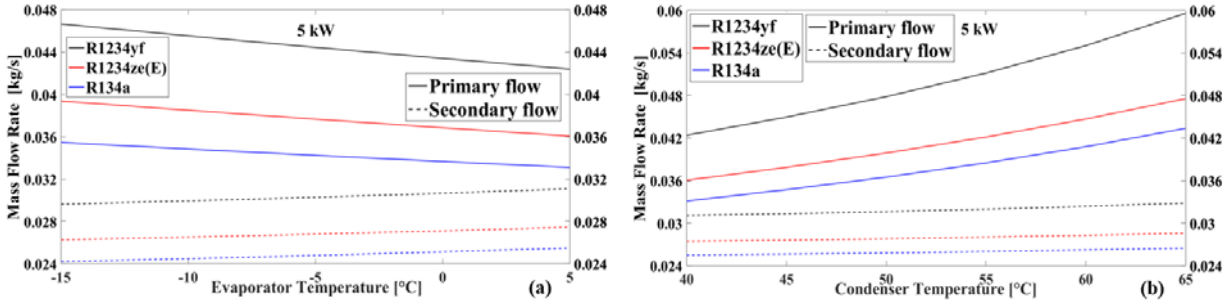

Fig. 6. Mass flow rates of the primary and secondary fluid flows for 5 kW cooling capacity at the optimum suction nozzle pressure with respect to the evaporator **(a)** and condenser **(b)** temperatures.

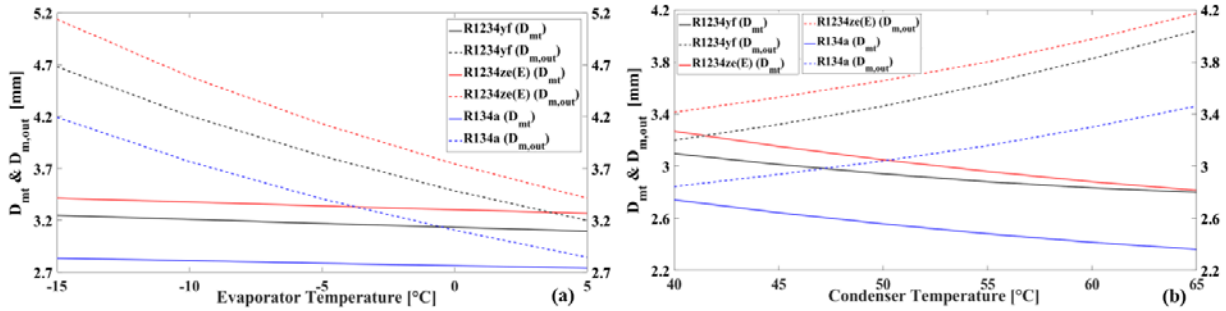

Fig. 7. Variation of the motive nozzle throat and outlet diameters according to the evaporator **(a)** and condenser **(b)** temperatures for a 5 kW experimental system.

In Fig. 8, the suction nozzle outlet diameter or the constant area mixing section diameter is presented for the same operating conditions. Hassanain et al. [8] defined both of the geometrical parameters separately. Mixing section diameter is affected mostly by the evaporator temperature. Although R1234yf and R1234ze(E) yield closer values for the motive nozzle throat and outlet diameters, R134a and R1234yf resulted in closer diameters in terms of mixing section diameter.

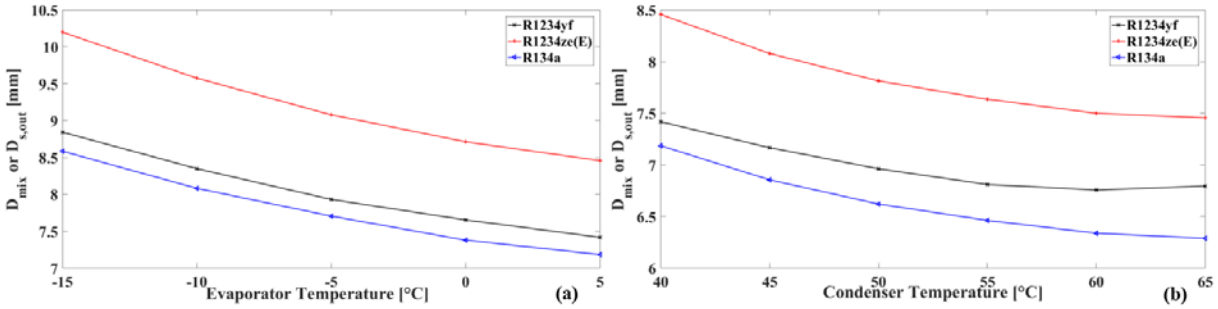

Fig. 8. Dependency of the constant area mixing section diameter (suction nozzle outlet diameter) on various evaporator **(a)** and condenser **(b)** temperatures for a 5 kW experimental system.

5 Conclusion

The main objective of this paper is to calculate the primary dimensions of a two-phase ejector for R1234yf, R1234ze(E), and R134a. First of all, the primary and secondary fluid mass flow rates are determined to calculate the aforecited design parameters. Effects of the evaporator and condenser temperatures on the secondary fluid mass flow rates are low and close to each other for the three refrigerants. Generally speaking, mass flow rate of R1234yf is more dependent on the changes in the operating temperatures when compared to the other investigated refrigerants.

Motive nozzle throat diameter changes more when condensation temperature is increased. However, motive and suction nozzle outlet diameters are more dependent on the evaporator temperature. Motive nozzle outlet diameter is the mostly affected geometrical parameter by the operating conditions. All geometrical calculations are given with reference to optimum suction nozzle pressure assumption figuring out the ideal operation of the ejector.

Acknowledgement

The authors would like to acknowledge the support of the Scientific and Technological Research Council of Turkey (TÜBİTAK) under Grant No: 116M367.

Nomenclature

h	Enthalpy [kJ/kg]
$\dot{m}$	Mass flow rate [kg/s]
P	Pressure [kPa]
$r(X_m)$	Quality or dry mass fraction [-]
s	Entropy [kJ/kgK]
T	Temperature [K]
$u(V)$	Velocity [m/s]
c	Sound velocity [m/s]
D	Diameter [mm]
η	Efficiency [-]
ρ	Density [kg/m^3]
α	Void fraction [-]
$L_{pre-mix}$	Length of the pre-mixing section

Subscripts

e	Evaporator
c	Condenser
$comp$	Compressor
in	Inlet
m	Primary (motive) nozzle/flow
opt	Optimum
out	Outlet
s	Suction (secondary) nozzle/flow
sc	Subcooling
sh	Superheating
g	Vapor
l	Liquid
mt	Motive nozzle throat
mix	Mixing section
tp	Two-phase mixture

References

1. S. Elbel, P. Hrnjak, *Ejector Refrigeration: An Overview of Historical and Present Developments with an Emphasis on Air-Conditioning Applications*. International Refrigeration and Air Conditioning Conference, Purdue University, USA (2008).
2. S. Elbel, N. Lawrence, *Review of recent developments in advanced ejector technology*, International Journal of Refrigeration, **62**, 1-18 (2016).
3. A.A. Kornhauser, *The use of an ejector as a refrigerant expander*, in: International Refrigeration and Air Conditioning Conference, Purdue University, USA (1990).
4. D.Q. Li, E.A. Groll, *Transcritical CO_2 refrigeration cycle with ejector-expansion device*, International Journal of Refrigeration **28**, 766-773 (2005).
5. S. Wongwises, S. Disawas, *Performance of the two-phase ejector expansion refrigeration cycle*, Technical note, International Journal of Heat and Mass Transfer **48**, 4282–4286 (2005).
6. P. Chaiwongsa, S. Wongwises, *Effect of throat diameters of the ejector on the performance of the refrigeration cycle using a two-phase ejector as an*

expansion device, International Journal of Refrigeration **30**, 601-608 (2007).

7. P. Chaiwongsa, S. Wongwises, *Experimental study on R-134a refrigeration system using a two-phase ejector as an expansion device,* Applied Thermal Engineering **28**, 467–477 (2008).
8. M. Hassanain, E. Elgendy, M. Fatouh, *Ejector expansion refrigeration system: Ejector design and performance evaluation*, International Journal of Refrigeration **58**, 1-13 (2005).
9. S.A. Sherif, W.E. Lear, J.M. Steadham, P.L. Hunt, J.B. Holladay, *Analysis and modeling of a two-phase jet pump of a thermal management system for aerospace applications,* International Journal of Mechanical Sciences **42**, 185-198 (2000).
10. REGULATION (EU) No 517/2014 OF THE EUROPEAN PARLIAMENT AND OF THE COUNCIL of 16 April 2014 on fluorinated greenhouse gases and repealing Regulation (EC) No 842/2006. Off. J. Eur. Union, 2014.
11. A.U. Atmaca, A. Erek, O. Ekren, *Impact of the mixing theories on the performance of ejector expansion refrigeration cycles for environmentally-friendly refrigerants*, International Journal of Refrigeration **97**, 211-225 (2019).
12. E.W. Lemmon, M.L. Huber, M.O. McLinden, 2013, NIST Standard Reference Database 23: Reference Fluid Thermodynamic and Transport Properties-REFPROP, Version 9.1, National Institute of Standards and Technology, Standard Reference Data Program, Gaithersburg.
13. M. Minnaert, XVI. *On musical air-bubbles and sounds of running water*, Philos. Mag. 16 (1933) 235–248.
14. S.L. Smith, *Void fractions in two-phase flow: a correlation based upon an equal velocity head model*, Proc. Inst. Mech. Eng. 184, 647–664 (1969).